Article

Not peer-reviewed version

Correlation-Based Single-Phase Heat Transfer Assessment of Binary HFE/Ethyl Acetate Mixtures in Minichannels

Artur Piasecki and Magdalena Piasecka *

Posted Date: 9 April 2026

doi: 10.20944/preprints202604.0657.v1

Keywords: binary mixtures; thermophysical properties; dielectric fluids; minichannel; heat transfer coefficient; Nusselt number; single-phase forced convection

Article

Correlation-Based Single-Phase Heat Transfer Assessment of Binary HFE/Ethyl Acetate Mixtures in Minichannels

Artur Piasecki [1] and Magdalena Piasecka [2,*]

[1] Faculty of Environmental Engineering, Geomatics and Renewable Energy, Kielce University of Technology, 25-314 Kielce, Poland

[2] Faculty of Mechatronics and Mechanical Engineering, Kielce University of Technology, 25-314 Kielce, Poland

* Correspondence: tmpmj@tu.kielce.pl; Tel.: +48-41-34-24-320

Abstract

This paper reports thermophysical-property data for binary dielectric mixtures of hydrofluoroether (HFE) fluids and ethyl acetate (EA) and applies a correlation-based workflow to compare their single-phase forced-convection performance in rectangular minichannels. Density, viscosity, thermal conductivity, and isobaric heat capacity were measured at three temperature levels (293.1, 313.1, and 328.1 K) for selected compositions of HFE-7100/EA, HFE-7300/EA, and HFE-73DE/EA. Using these measured properties, Reynolds and Prandtl numbers were evaluated and a laminar thermally developing correlation was employed to obtain Nusselt numbers and corresponding heat transfer coefficients. The assessment was performed for two geometries representing a long reference minichannel module and a short multi-minichannel module. A validation dataset for pure HFE-7100 in the short module, derived from IR thermography and an energy-balance data reduction, indicates a systematic deviation between correlation-based estimates and experimental values, which should be considered when interpreting absolute predictions. The presented dataset and workflow support transparent down-selection of candidate mixtures prior to extended experimental campaigns.

Keywords: binary mixtures; thermophysical properties; dielectric fluids; minichannel; heat transfer coefficient; Nusselt number; single-phase forced convection

1. Introduction

Heat exchangers are key components of thermal systems, spanning refrigeration and air conditioning, high-power electronics cooling, cryogenic technologies, photovoltaics, and industrial installations. Their performance depends strongly on the choice of working fluid, whose thermophysical properties must fit the application constraints, including temperature range, operating pressure, flow regime (laminar or turbulent), as well as chemical compatibility and operational safety. Fluorinated liquids-such as HFE (hydrofluoroethers), PFPE (perfluoropolyethers), and FC (Fluorinerts) - are increasingly used due to their low electrical conductivity, high chemical and thermal stability, and wide atmospheric-pressure boiling ranges (from ~300 K to above 500 K), which is attractive for cooling electronic and optoelectronic components. However, their thermal conductivity is typically low and their cost can be high, motivating the development of mixtures that allow fluid properties to be tailored to specific process needs. Binary mixtures of fluorinated liquids with organic solvents or other fluorinated fluids are therefore widely investigated as tunable alternatives to ionic liquids and nanofluids, enabling adjustment of boiling temperature, density, viscosity, and heat capacity while maintaining compatibility with common materials and pumping systems.

 doi:10.20944/preprints202604.0657.v1

The paper [1] extends differential scanning calorimetry (DSC) to obtain atmospheric-pressure boiling-point/VLE data for binary mixtures with large boiling-point differences by optimizing key process parameters (sample volume and heating rate) to mitigate pre-evaporation artifacts. It demonstrates the approach on several test systems and then applies it to the previously unreported carvacrol–DMSO mixture, correlating the measured boiling line with the NRTL model (including evidence of strong non-ideality/azeotropic behavior).

Recent modelling and data-driven approaches have been proposed for HFE-containing systems. Aminian et al. [2] modelled the ideal-gas heat capacity and critical properties of hydrofluoroethers from the HFE-7000–7500 series using ab initio methods combined with Peng–Robinson equations of state. Urata et al. [3] proposed an artificial-neural-network model to predict vapour–liquid equilibria in HFE-containing systems. Wu et al. [4] introduced a machine learning-based group contribution model for estimating critical temperatures of binary refrigerant mixtures from molecular structure, while Soria-Lopez et al. [5] showed that ML algorithms can outperform classical viscosity mixing rules for binary alkane mixtures, effectively capturing nonlinear composition–viscosity relationships.

High-quality high-pressure datasets are also available: Muñoz-Rujas et al. [6] investigated the thermophysical properties of binary HFE-7200 + 2-propanol mixtures over 0.1–140 MPa and 293.15–393.15 K, correlating density with a Tait-type equation, deriving derivative properties, and reporting sound speeds at 0.1 MPa. In a related study [7], sound speed and density data were reported for HFE-7500 + diisopropyl ether mixtures up to 100 MPa. Ogawa et al. [8] analysed the thermodynamic properties of hydrofluoroether mixtures with selected organic solvents and reported positive excess molar volumes and composition-dependent excess enthalpies.

From the application perspective, Xu et al. [9] demonstrated that zeotropic, partially immiscible mixtures in pulsating heat pipes can form emulsions that enhance heat transfer. Eissa et al. [10] developed a generalised non-equilibrium heat transfer model for predicting flow condensation of binary zeotropic mixtures, integrating vapour-phase mass diffusion and interfacial temperature coupling; validated against 871 experimental data points, it showed excellent agreement (92% within ±30%), offering a robust tool for compact heat exchanger design.

Tagliaferri et al. [11] showed that, for CFD of bubbling fluidized bidisperse mixtures, a first-order upwind discretization can introduce strong numerical diffusion that suppresses bubble holdup and mixing, whereas a second-order upwind scheme yields more realistic bubble dynamics and correctly predicts the transition to a fully mixed state; the restitution coefficient has a minor influence except near the quasi-ideal value $e \approx 0.99$, and explicit vs implicit time integration mainly affects the transient duration rather than the pseudo-steady behaviour.

Other researchers have examined complementary aspects of binary mixtures, including molecular interactions, phase behaviour, and interfacial phenomena. Verma et al. [12] reported strong donor–acceptor interactions in ether/hydrocarbon mixtures based on density, ultrasonic velocity, and refractive index data, while Tsai et al. [13] benchmarked molecular dynamics predictions of transport properties for alcohol/water mixtures, identifying force-field combinations that best reproduce diffusion and density trends.

In previous work [14], the authors combined thermophysical property measurements with validated conjugate CFD to assess HFE-73DE/ethyl acetate mixtures for laminar minichannel cooling and to identify compositions offering a heat-transfer/pressure-drop compromise.

This paper provides a transparent, correlation-based workflow to translate these measured properties into comparable single-phase forced-convection heat-transfer indicators for rectangular minichannels. The novelty lies in combining a dedicated property dataset for HFE/EA mixtures with a consistent minichannel assessment framework applied to two representative module geometries, and in anchoring the assessment with an independent validation dataset for pure HFE-7100 obtained in the short multi-minichannel module using IR thermography and an energy-balance data reduction.

 doi:10.20944/preprints202604.0657.v1

2. Characteristics of Pure Liquids and Selected Binary Mixtures

The present study considers three binary mixture series based on hydrofluoroethers (HFEs) and an organic ester: HFE-7100/EA, HFE-7300/EA, and HFE-73DE/EA. These liquids were selected because they are electrically insulating, chemically stable, and relevant to thermal-management and compact heat-exchanger applications, while the ester co-solvent enables tunability of density, viscosity, and boiling behaviour.

Table 1 provides typical reference properties of the base fluids (reported at 298 K unless stated otherwise). For HFE-7100 [15] and HFE-7300 [16], manufacturer data indicate boiling points of 334.1 K and 371.1 K, respectively, and low viscosities, which are favourable for achieving moderate Reynolds numbers in minichannels at practical mass fluxes. For HFE-73DE [17], the boiling point is approximately 321.1 K and the viscosity is low. Ethyl acetate [18] exhibits a normal boiling temperature of about 350.2 K and a liquid isobaric heat capacity near 298 K of ~169 J/(mol·K), which corresponds to ~1.9 kJ/(kg·K); complementary transport-property tables are available from compiled chemical-property sources.

Table 1. Selected physical properties of the base fluids.

Physical properties	HFE-7100	HFE-7300	HFE-73DE	EA
Density, kg/m³	1520	1660	1280	902
Viscosity, mm²/s	0.401	0.71	0.403	0.463
Thermal conductivity, W/(m·K)	0.069	0.063	0.075	0.149
Specific heat, J/(kg·K)	1172	1140	1020	2020
Boiling temperature, K	334.1	371.1	321.1	350.2

The mass fractions of the HFE-7100/EA, HFE-7300/EA, and HFE-73DE/EA mixtures considered in the analysis were 10/90, 25/75, 50/50, and 75/25 at three temperature levels. The 10/90 composition was available for HFE-73DE/EA and HFE-7100/EA only. The 75/25 composition of HFE-73DE/EA was excluded at all three temperatures due to physically inconsistent property values that could not be independently verified; no correction was applied. The measured thermophysical properties of the remaining mixtures and compositions were used as inputs to the correlation-based calculations and are reported in the corresponding tables.

3. Experimental Rig and Minichannel Modules

3.1. General Information

The present study comprises (i) a correlation-based assessment of selected binary mixtures using experimentally measured mixture properties, performed for two minichannel modules - a long reference module (Setup #1) and a short multi-minichannel module (Setup #2), and (ii) an experimental validation dataset acquired in the short module (Setup #2) using a pure reference fluid (HFE-7100). For the flow of either mixtures or pure liquids in the single minichannel (Setup #1) or in the central minichannel of the parallel-channel group (Setup #2), laminar single-phase forced convection was assumed.

The configuration with a long minichannel (Setup #1) was used in earlier experimental studies by the authors, in which liquid crystal thermography was applied to measure the temperature of the outer surface of the heated foil; however, those data were not used in the present analysis [19].

The configuration with a short minichannel module (Setup #2) was used in recent experimental studies by the authors, in which infrared thermography was employed to measure the temperature of the outer surface of the heated foil [20]. These IR-based data were selected for the present analysis because they provide a more complete and reliable wall-temperature field. In the liquid-crystal thermography measurements, portions of the foil surface could not be evaluated when the local

 doi:10.20944/preprints202604.0657.v1

temperature fell outside the active temperature range of the liquid-crystal coating; therefore, this technique was not adopted for the validation dataset used here.

An uncertainty analysis of the key measured quantities was presented in [19,20]. The uncertainty of the determined heat transfer coefficient is strongly dependent on the accuracy of the temperature measurement.

It should also be noted that the mixtures addressed in this article were not tested experimentally in the heat-transfer rig. Therefore, the heat transfer coefficients and Nusselt numbers reported for the mixtures are calculated estimates obtained from the measured thermophysical properties and a selected literature correlation, applied to the geometries and operating assumptions defined in this work.

3.2. Experimental Rig with a Minichannel Module

The validation experiments were performed in single-phase forced convection. The working fluid was circulated through the test section at controlled inlet temperature and mass flow rate, while the heat input was supplied electrically at the heated wall of the minichannel module (Setup #2). Inlet/outlet temperatures and pressures were recorded continuously, and the wall-temperature field on the outer surface of the heater foil was measured by infrared (IR) thermography, providing a spatially resolved temperature distribution along the observation length. The validation dataset for the reference fluid (HFE-7100) was collected using Setup #2.

A schematic of the experimental loop and the interchangeable test sections is shown in Figure 1.

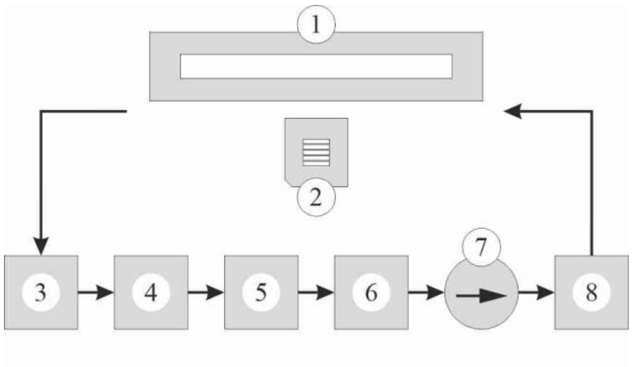

Figure 1. A scheme of experimental stand: 1 - setup #1 (long module with the minichannel); 2 - setup #2 (short module with the 5 minichannels); 3 - condenser; 4 - pressure-control unit; 5 - deaerator; 6 - filter; 7 - pump; 8 – mass flow meter.

In the rig, the pump delivered the working fluid to a pressure-control unit that also served as an expansion volume. The liquid occupied one side of the vessel, while compressed air on the opposite side maintained the set system pressure. Downstream of the pressure-control unit, the fluid passed through a preheater to reach the desired inlet temperature (typically close to, but below, the saturation temperature) before entering the test section. A detailed description of the experimental facility is provided in [19,20].

The measurements were conducted under steady-state conditions at different levels of electrical power supplied to the heater, resulting in a set of imposed heat-flux levels.

3.3. Reference Minichannel Modules

Both modules comprise minichannels with a depth of 1 mm. In each minichannel, the heated wall was formed by a Haynes-230 foil with a thickness of approximately 0.1 mm, the opposite wall was a glass window, and the side walls were made of PTFE. This work focuses on the short module with five parallel minichannels (Setup #2), which is schematically shown in Figure 2.

 doi:10.20944/preprints202604.0657.v1

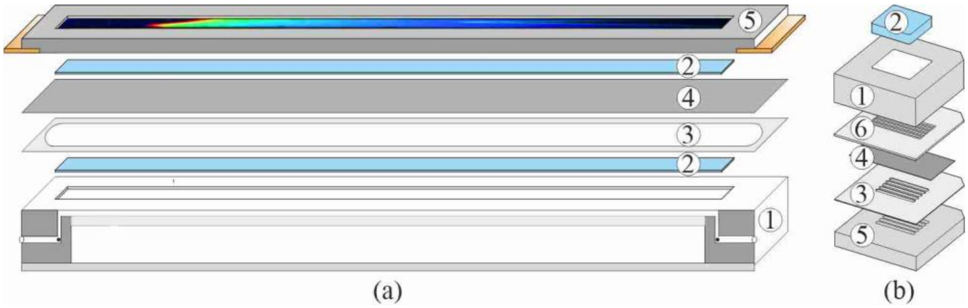

Figure 2. Schematic diagrams of: (a) the long module with a single minichannel (Setup #1); (b) the short module with five parallel minichannels (Setup #2); 1 – body, 2 – glass plate, 3 – PTFE minichannel insert, 4 – heated foil, 5 – cover plate, 6 – PTFE electrically insulating insert.

The principal geometrical dimensions of both modules are summarized in Table 2. Setup #1 employs a single minichannel with a length of 0.36 m, whereas Setup #2 uses five parallel minichannels, each 0.043 m long; in both modules, the minichannel depth is 1 mm.

Table 2. Geometrical characteristics of the test modules.

	Setup #1	**Setup #2**
Number of minichannels (-)	1	5
Minichannel length L (m)	0.36	0.043
Minichannel width w (m)	0.004	0.006
Minichannel depth s (m)	0.001	0.001

4. Calculations and Correlation-Based Assessment Method

4.1. Correlation-Based Assessment of Single-Phase Forced Convection

To compare selected mixtures of HFE-7100, HFE-7300, HFE-73DE and ethyl acetate (EA) under identical hydraulic conditions and a fixed operating point, a correlation-based assessment approach was adopted for single-phase forced convection in a reference rectangular minichannel. The assessment geometry and operating point were fixed as: channel width w = 0.004 m, channel depth s = 0.001 m, length L = 0.36 m, hydraulic diameter D_h = 1.6 mm and mass flux G = 200 kg/(m²·s).

All thermophysical properties of the mixtures were determined at the Faculty of Civil Engineering, Mechanics and Petrochemistry, Warsaw University of Technology in Płock (Poland). The dataset was collected at three temperature levels (293.1, 313.1, and 328.1 K) and the measured properties were treated as constant at each level for subsequent analysis and modelling. Details of the property-measurement methods are given in [14].

For each mixture and temperature, the dynamic viscosity was computed from density and kinematic viscosity. The Reynolds and Prandtl numbers were then calculated according to following dependences:

$$Re = \frac{G \cdot D_h}{\mu} \tag{1}$$

$$Pr = \frac{\mu c_p}{k} \tag{2}$$

where μ is the dynamic viscosity, c_p is the specific heat and k is the thermal conductivity of the fluid.

The average Nusselt number was estimated using the classical Sieder–Tate type correlation [21] for laminar internal flow with thermal development effects:

$$Nu = 1.86\left(Re \cdot Pr \cdot \frac{D_h}{L}\right)^{\frac{1}{3}}\left(\frac{\mu}{\mu_w}\right)^{0.14} \tag{3}$$

where L is the heated length of the minichannel.

doi:10.20944/preprints202604.0657.v1

The viscosity ratio $\left(\frac{\mu}{\mu_w}\right)^{0.14}$ is the Sieder–Tate correction accounting for property variations between the bulk fluid and the wall: μ is the dynamic viscosity evaluated at the bulk (mean) fluid temperature, while μ_w is the dynamic viscosity evaluated at the wall temperature. In the present calculations, this viscosity ratio correction was not applied and ($\mu/\mu_w{}^{0.14}$) was set to unity. This is equivalent to assuming a small viscosity variation across the thermal boundary layer or using a bulk-property approximation at each temperature level. The use of the hydraulic diameter to extend tube correlations to non-circular ducts is standard practice in preliminary internal-flow heat transfer estimates, while detailed aspect-ratio-dependent solutions for fully developed laminar duct flow can be found in dedicated duct-flow sources [22].

Finally, the heat transfer coefficient was obtained from the definition of the Nusselt number ($Nu=h\cdot D_h/k$). Using the Sieder–Tate correlation to compute Nu_{corr}, the corresponding coefficient is

$$h_{corr} = \frac{Nu\cdot k}{D_h} \tag{4}$$

where k is the thermal conductivity evaluated at the bulk (reference) fluid temperature.

The assessment is restricted to single-phase forced convection with no phase change, no conjugate heat conduction in the wall, and no pressure-drop constraint included in the ranking criterion. Properties are evaluated at discrete temperatures (293.1/313.1/328.1 K) and assumed uniform for each case. The adopted correlation targets laminar flow with thermal development along the heated length; therefore, the computed Nu and h should be interpreted as comparative indicators under the specified geometry and operating point, suitable for experimental validation.

5. Results and Analysis

5.1. Heat-Transfer Assessment Outputs For Investigated Mixtures

This section presents the measured thermophysical-property trends and the resulting heat-transfer assessment outputs for the investigated mixtures.

For each mixture series (HFE-7100/EA, HFE-7300/EA, and HFE-73DE/EA), mixtures were considered at selected mass fractions (first component/second component) and characterised at 293.1, 313.1, and 328.1 K under near-atmospheric pressure. The measured dataset includes density, kinematic viscosity, thermal conductivity and specific heat capacity. Table 3 summarises the measured properties at 293.1 K, Table 4 shows the measured properties at 313.1 K, Table 5 presents the measured properties at 328.1 K. It should be added that the 75/25 composition of HFE-73DE/EA was excluded from further analysis at all three temperature levels because the reported property set for this mass fraction exhibited internal inconsistencies (e.g., non-physical trends relative to neighbouring compositions and/or values exceeding those of the pure components) and could not be confirmed by repeat measurements. No correction was applied.

Within the analysed composition ranges, the properties vary systematically with both temperature and composition, indicating that these mixtures can be used to tailor transport and thermal characteristics for compact heat-transfer devices.

Table 3. Summary of measured properties and assessment outputs for all selected mixtures and compositions retained for analysis at T = 293.1 K (reference Setup #1: w = 4 mm, s = 1 mm, L = 0.36 m, D_h = 1.6 mm, G = 200 kg/(m² s)).

Mixture	Mass fraction (%)	ρ (kg/m³)	μ (mPa·s)	c_p (J/(kg·K))	k (W/(m·K))	Re (–)	Nu_{corr} (–)	h_{corr} (W/(m²·K))
HFE-73DE/EA	10/90	931	0.4731	503.8	0.165	676.4	3.0345	312.9
HFE-73DE/EA	25/75	969	0.4877	313.3	0.189	656.2	2.4755	292.4
HFE-73DE/EA	50/50	1035	0.4839	444.6	0.207	661.2	2.6988	349.2
HFE-7100/EA	10/90	940	0.5194	1348.3	0.125	616.1	4.6216	361.1
HFE-7100/EA	25/75	1017	0.5039	573.6	0.116	635.0	3.5636	258.4

Preprints.org (www.preprints.org) | NOT PEER-REVIEWED | Posted: 9 April 2026 doi:10.20944/preprints202604.0657.v1

HFE-7100/EA	50/50	1111	0.5341	443.6	0.105	599.1	3.3814	221.9
HFE-7100/EA	75/25	1216	0.5787	354.5	0.089	553.0	3.3157	184.4
HFE-7300/EA	25/75	1006	0.5005	431.1	0.133	639.3	3.0956	257.3
HFE-7300/EA	50/50	1154	0.578	374.2	0.101	553.7	3.2367	204.3
HFE-7300/EA	75/25	1348	0.741	328.6	0.087	431.8	3.2575	177.1

Table 4. Summary of measured properties and assessment outputs for all selected mixtures and compositions retained for analysis at $T = 313.1$ K.

Mixture	**Mass fraction (%)**	**ρ (kg/m³)**	**μ (mPa·s)**	**c_p (J/(kg·K))**	**k (W/(m·K))**	**Re (–)**	**Nu_{corr} (–)**	**h_{corr} (W/(m²·K))**
HFE-73DE/EA	10/90	902.1	0.3804	841.6	0.155	841.1	3.6764	356.2
HFE-73DE/EA	25/75	951.7	0.399	430.6	0.177	802.0	2.8132	311.2
HFE-73DE/EA	50/50	933.0	0.3613	523.6	0.194	885.7	2.9123	353.1
HFE-7100/EA	10/90	888.0	0.3719	1464.6	0.123	860.5	4.7765	367.2
HFE-7100/EA	25/75	785.2	0.3239	676.5	0.111	987.8	3.8208	265.1
HFE-7100/EA	50/50	1044.0	0.4143	486.3	0.1	772.5	3.5438	221.5
HFE-7100/EA	75/25	1042.3	0.4158	407.1	0.082	769.6	3.5683	182.9
HFE-7300/EA	25/75	1067.4	0.4475	543.5	0.107	715.1	3.5956	240.5
HFE-7300/EA	50/50	1138.0	0.4603	415.8	0.095	695.2	3.4215	203.2
HFE-7300/EA	75/25	1470.8	0.6413	359.1	0.08	499.0	3.4505	172.5

Table 5. Summary of measured properties and assessment outputs for all selected mixtures and compositions retained for analysis at $T = 328.1$ K.

Mixture	**Mass fraction (%)**	**ρ (kg/m³)**	**μ (mPa·s)**	**c_p (J/(kg·K))**	**k (W/(m·K))**	**Re (–)**	**Nu_{corr} (–)**	**h_{corr} (W/(m²·K))**
HFE-73DE/EA	10/90	894.4	0.3292	1356.2	0.148	972.0	4.3771	404.9
HFE-73DE/EA	25/75	951.6	0.3543	613.2	0.169	903.2	3.2142	339.5
HFE-73DE/EA	50/50	916.3	0.3478	680.3	0.185	920.0	3.2286	373.3
HFE-7100/EA	10/90	888.0	0.327	1599.9	0.12	978.6	4.9599	372.0
HFE-7100/EA	25/75	766.3	0.2802	797.0	0.11	1142.2	4.0475	278.3
HFE-7100/EA	50/50	1030.0	0.3594	563.1	0.097	890.4	3.7593	227.9
HFE-7100/EA	75/25	1022.0	0.3431	542.0	0.081	932.6	3.9416	199.5
HFE-7300/EA	25/75	1084.0	0.4036	717.5	0.097	792.9	4.0755	247.1
HFE-7300/EA	50/50	1107.2	0.3906	496.7	0.093	819.3	3.6563	212.5
HFE-7300/EA	75/25	1458.6	0.5479	369.4	0.073	584.0	3.5911	163.8

5.2. Thermophysical Property Trends

Across all mixture series, density decreases with temperature and changes systematically with composition. Kinematic viscosity decreases with increasing temperature and typically varies non-linearly with composition. Thermal conductivity and specific heat capacity also show composition dependence, which is essential for predicting Prandtl number and, consequently, convective heat-transfer performance.

5.3. Correlation-based Assessment Results for Setup #1 (Long Test Section)

The long-channel assessment (Tables 3–5), together with Figure 3, shows clear differences between mixture families within the compositions retained for analysis. Under the fixed reference operating point, EA-rich compositions generally yield higher correlation-based heat-transfer coefficients. This trend reflects the combined influence of viscosity (via the Reynolds number) and thermal conductivity (via the *Nu*–*h* conversion) at each temperature level.

For the HFE-7100/EA family, the highest h_{corr} values occur at the most EA-rich composition available (10/90) across the investigated temperature range. For HFE-73DE/EA, the ranking is limited

doi:10.20944/preprints202604.0657.v1

to 10/90–50/50 because the 75/25 composition was excluded; within the retained set, the EA-rich 10/90 case becomes the highest at 328.1 K, whereas at 293.1 and 313.1 K the differences between the available compositions are smaller. For HFE-7300/EA, the comparison is restricted to the compositions available in the dataset (25/75–75/25).

Using the reference geometry and operating point defined in Section 4, Reynolds and Prandtl numbers were computed for each mixture at 293.1, 313.1, and 328.1 K. In the investigated range, an increase in temperature generally enhances h_{corr}, primarily through viscosity reduction (higher *Re*), while the temperature dependence of thermal conductivity is comparatively weaker. Figure 3 summarizes the correlation-based Nusselt number and heat-transfer coefficient as functions of mass fraction under the Setup #1 reference conditions.

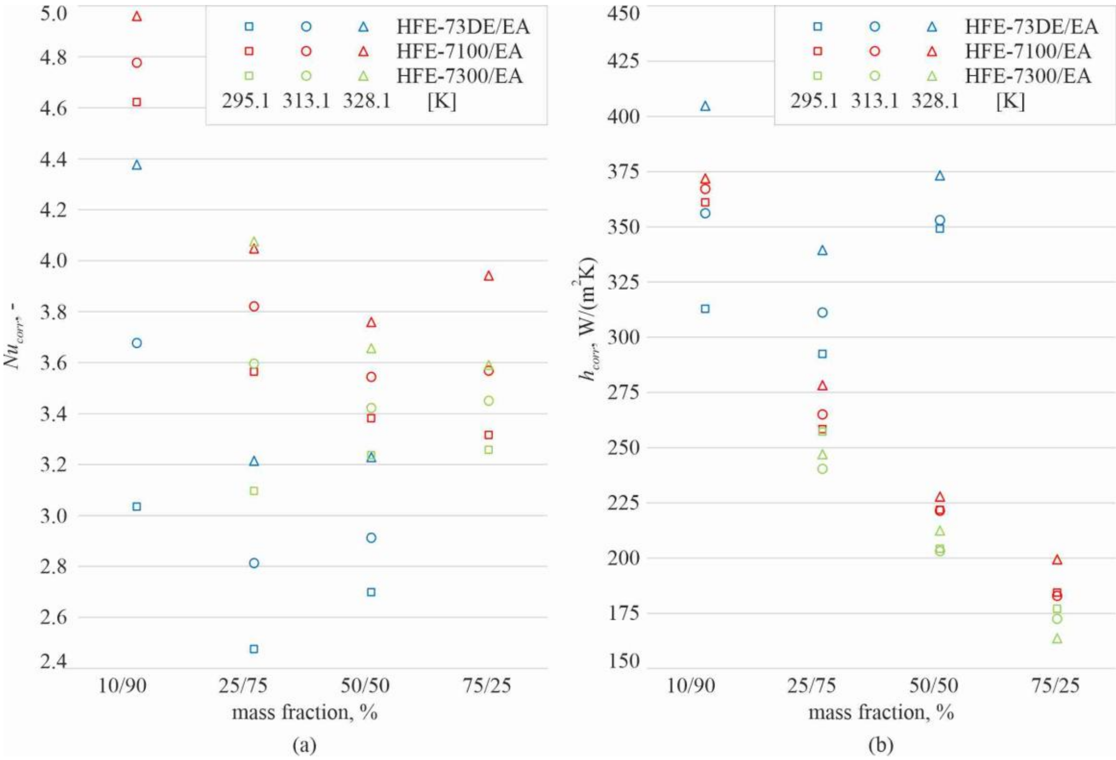

Figure 3. Correlation-based estimates under the Setup #1 reference conditions: (a) Nusselt number versus mass fraction; (b) heat transfer coefficient versus mass fraction for the binary mixtures.

5.4. Correlation-Based Assessment Results for Setup #2 (Short Test Section)

For the short-module geometry, the same correlation framework was applied using the module-specific hydraulic diameter and heated length. In contrast to the long-module assessment, the mass flux was set to the value corresponding to the selected convection-only operating point used for validation (Section 6). This ensures that the correlation-based estimates for Setup #2 are evaluated under the same hydraulic conditions as the experimental dataset, enabling a consistent comparison.

For the Setup #2 assessment (Tables 6–8 and Figure 4), the reference conditions were defined by the Setup #2 geometry (five parallel minichannels with w = 0.006, s = 0.001 m, and L = 0.043 m; Table 2). The hydraulic diameter was evaluated accordingly, and mixture properties at each temperature level were treated as constant reference values, in analogy to the long-module calculations. Based on the experimental operating conditions, a fixed mass flux of G = 372.5 (kg/(m^2·s) was adopted.

Tables 6–8 compile the correlation-based assessment outputs for the selected mixtures and compositions retained for analysis under the Setup #2 reference conditions at T = 293.1, 313.1, and 328.1 K. Figure 4 illustrates the corresponding Nusselt number and heat-transfer coefficient as functions of mass fraction for the binary mixtures under the same Setup #2 reference conditions.

Table 6. Summary of correlation-based assessment outputs for the selected mixtures and compositions retained for analysis at T = 293.1 K under the Setup #2 reference conditions.

Mixture	Mass fraction (%)	*Re* (–)	Nu_{corr} (–)	h_{corr} (W/(m²·K))
HFE-73DE/EA	10/90	1939.7	11.1955	966.5
HFE-73DE/EA	25/75	1802.4	8.2211	810.5
HFE-73DE/EA	50/50	1836.0	8.2579	891.2
HFE-7100/EA	10/90	1952.9	12.6861	888.0
HFE-7100/EA	25/75	2279.3	10.3525	664.3
HFE-7100/EA	50/50	1776.9	9.6153	544.1
HFE-7100/EA	75/25	1861.0	10.0816	476.4
HFE-7300/EA	25/75	1582.3	10.4242	589.8
HFE-7300/EA	50/50	1635.0	9.3518	507.3
HFE-7300/EA	75/25	1165.5	9.1851	391.1

Table 7. Summary of correlation-based assessment outputs for the selected mixtures and compositions retained for analysis at T = 313.1 K under the Setup #2 reference conditions.

Mixture	Mass fraction (%)	*Re* (–)	Nu_{corr} (–)	h_{corr} (W/(m²·K))
HFE-73DE/EA	10/90	1678.5	9.4033	850.2
HFE-73DE/EA	25/75	1600.4	7.1955	742.9
HFE-73DE/EA	50/50	1767.4	7.4489	843.0
HFE-7100/EA	10/90	1717.2	12.2169	876.6
HFE-7100/EA	25/75	1971.2	9.7725	632.8
HFE-7100/EA	50/50	1541.5	9.0641	528.7
HFE-7100/EA	75/25	1535.8	9.1268	436.6
HFE-7300/EA	25/75	1426.9	9.1967	574.0
HFE-7300/EA	50/50	1387.3	8.7514	485.0
HFE-7300/EA	75/25	995.8	8.8254	411.9

Table 8. Summary of correlation-based assessment outputs for the selected mixtures and compositions retained for analysis at T = 328.1 K under the Setup #2 reference conditions.

Mixture	Mass fraction (%)	*Re* (–)	Nu_{corr} (–)	h_{corr} (W/(m²·K))
HFE-73DE/EA	10/90	1349.9	7.7616	747.1
HFE-73DE/EA	25/75	1309.4	6.3318	698.1
HFE-73DE/EA	50/50	1319.5	6.9028	833.5
HFE-7100/EA	10/90	1229.5	11.8209	861.9
HFE-7100/EA	25/75	1267.1	9.1147	616.8
HFE-7100/EA	50/50	1195.5	8.6489	529.7
HFE-7100/EA	75/25	1103.5	8.4807	440.3
HFE-7300/EA	25/75	1275.8	7.9177	614.3
HFE-7300/EA	50/50	1104.9	8.2785	487.7
HFE-7300/EA	75/25	861.7	8.3318	422.8

The resulting Tables 6–8 and Figure 4 confirm that the down-selection is not an artifact of the long-channel assumptions. In particular, mixtures that minimize viscosity while preserving sufficiently high thermal conductivity remain favoured. The validation presented in Section 6 shows that the correlation slightly overpredicts heat transfer coefficient h_{corr} for HFE-7100 under the tested conditions, which should be considered when interpreting absolute values; however, the relative ranking is expected to be preserved.

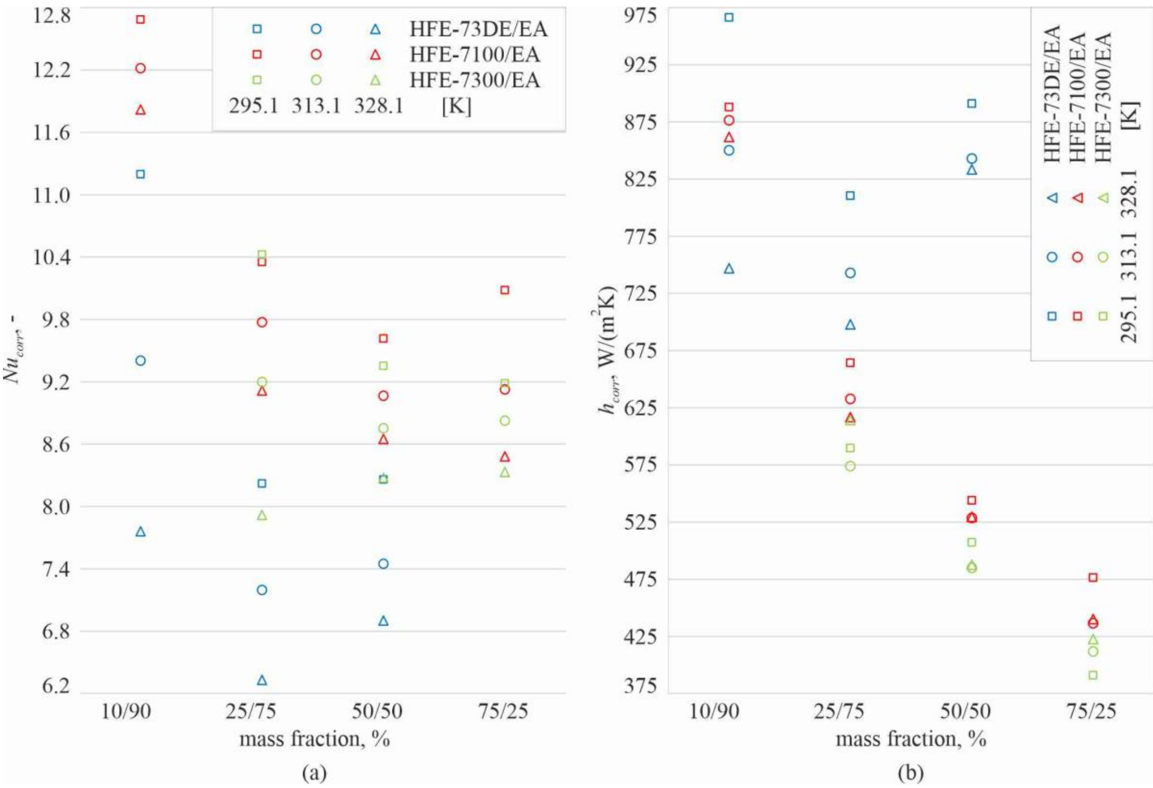

Figure 4. Correlation-based estimates under the Setup #2 reference conditions: (a) Nusselt number versus mass fraction; (b) heat transfer coefficient versus mass fraction for the binary mixtures.

6. Validation of the Correlation-Based Estimates Against the Experimental Dataset

The correlation-based estimates were validated against an experimental dataset obtained for pure HFE-7100 in the short multi-minichannel module (Setup #2, five parallel minichannels) under single-phase forced convection. The selected convection-only operating point corresponded to a mean mass flux of G_{mean} = 372.5 (kg/(m²·s)), inlet and outlet bulk-fluid temperatures of $T_{f,in}$= 287.3 K and $T_{f,in}$= 288.5 K, inlet and outlet gauge pressures of p_{in} = 25559.9 Pa and p_{out} = 24399.2 Pa, and an imposed heat flux of $q^{''}$ = 6473.2 W/m² calculated from the measured electrical current and voltage. The IR-measured outer-foil temperature ranged from 294.7 K to 303.7 K; the ambient-air temperature was 294.9 K and the atmospheric pressure was 0.96 bar.

The experimental heat transfer coefficient was evaluated from the spatial wall-temperature field measured by IR thermography. For each frame, the local coefficient was computed as

$$h_{exp}(x) = \frac{q^{''}}{[T_F(x) - T_f(x) - \Delta T_{cond}]} \quad (5)$$

where $T_F(x)$ is the local outer-surface temperature of the heated foil measured by infrared thermography, $T_f(x)$ is the linear HFE-7100 bulk-temperature profile between the measured inlet/outlet temperatures (measured by K-type thermocouples placed in the inlet and outlet of the minichannel collector), $q^{''}$ is determined from the measured current and voltage, the heated area, and the assumed heat-loss correction.

Furthermore, ΔT_{cond} accounts for conduction through the heater foil and is calculated as follows:

$$\Delta T_{cond} = \frac{q^{''} \cdot \delta_F}{k_F} \quad (6)$$

where δ_F is the heater foil thickness and k_F means foil conductivity.

A minimal quality criterion was applied (temperature difference in Equation (5) > 0.5 K and h_{exp} > 0), and $h_{exp,mean}$ was obtained by averaging over the retained axial positions. The correlation-based

 doi:10.20944/preprints202604.0657.v1

heat transfer coefficient h_{corr} was computed by first evaluating Re and Pr from Eqs. (1)–(2), then calculating Nu_{corr} using the laminar thermally developing correlation (3), and finally converting Nu_{corr} to h_{corr}. For this first-stage validation, μ, c_p and k were treated as constant reference values for HFE-7100 (near 298.1 K). For the selected 30 low-heat-flux frames (convection-only subset), the mean $h_{exp,mean}$ was 480.6 ± 11.7 W/(m² K), while the mean h_{corr} was 555.2 ± 0.1 W/(m² K). The mean relative difference was defined as

$$\Delta h_{rel} = \frac{(h_{exp} - h_{corr})}{h_{corr}} \cdot 100\%, \quad (7)$$

and equalled -13.44% (median −14.15%; 10th–90th percentiles −15.23% to −10.72%). The RMSE was 75.5 W/(m² K) and the MAPE (relative to h_{exp}) was 15.6%.

Table 9 lists the 30 low-heat-flux (convection-only) validation cases for Setup #2, including the mass flux G, imposed heat flux q'', the experimentally obtained mean heat transfer coefficient $h_{exp,mean}$, the corresponding correlation-based value h_{corr}, and the resulting relative difference Δh_{rel}.

Table 9. Validation dataset for the short module (Setup #2, HFE-7100): experimental mean heat transfer coefficient $h_{exp,mean}$, compared with the correlation-based value h_{corr} calculated using Equation (3), and the resulting relative difference Δh_{rel} calculated from Equation (7).

G (kg/(m²s))	q'' (W/m²)	$h_{exp,mean}$ (W/(m²K))	h_{corr} (W/(m²K))	Δh_{rel} (%)
372.2	4291.5	470.8	555.1	-15.2
372.1	4859.2	503.8	555.1	-9.2
372.2	5773.7	520.7	555.1	-6.2
372.7	6144.2	470.8	555.4	-15.2
372.4	6163.8	473.2	555.2	-14.8
372.4	6169.3	476.4	555.2	-14.2
372.1	6176.0	468.1	555.1	-15.7
372.3	6181.7	478.1	555.2	-13.9
372.1	6181.8	478.4	555.1	-13.8
372.4	6184.6	475.9	555.2	-14.3
372.5	6186.8	473.3	555.3	-14.8
372.3	6187.8	466.8	555.2	-15.9
372.6	6198.7	475.1	555.3	-14.4
372.5	6199.8	473.5	555.3	-14.7
372.5	6208.4	476.0	555.3	-14.3
372.5	6209.7	482.0	555.3	-13.2
372.6	6210.7	480.9	555.3	-13.4
372.3	6214.7	476.8	555.2	-14.1
372.4	6217.4	470.6	555.2	-15.2
372.4	6220.7	476.3	555.2	-14.2
372.3	6223.7	489.1	555.2	-11.9
372.6	6226.7	502.6	555.3	-9.5
372.4	6227.8	479.5	555.2	-13.6
372.0	6229.8	487.1	555.0	-12.2
372.4	6230.8	475.2	555.2	-14.4
372.4	6232.8	474.1	555.2	-14.6
372.7	6232.8	480.5	555.4	-13.5
372.6	6241.8	484.5	555.3	-12.8
372.6	6242.5	482.6	555.3	-13.1
372.5	6247.8	495.0	555.3	-10.9

 doi:10.20944/preprints202604.0657.v1

7. Conclusions

Thermophysical-property data were compiled for three binary HFE/ethyl acetate systems (HFE-7100/EA, HFE-7300/EA, and HFE-73DE/EA) at 293.1, 313.1, and 328.1 K, providing consistent inputs for comparative single-phase forced-convection analysis in minichannel geometries.

A correlation-based assessment framework was implemented under fixed hydraulic assumptions. At each temperature level, the measured properties were treated as constant reference values to evaluate the relevant similarity numbers and to calculate Nusselt numbers and heat transfer coefficients using a laminar thermally developing correlation.

The assessment was carried out for two representative geometries (a long single-minichannel reference module and a short multi-minichannel module). Using both geometries reduces reliance on a single reference size and enables examination of the sensitivity of correlation-based estimates to channel dimensions.

Validation based on the short-module dataset for pure HFE-7100, obtained from IR thermography combined with an energy-balance data reduction, indicates a systematic deviation between correlation-based and experimental heat transfer coefficients within the convection-only subset. Accordingly, the calculated values are most appropriately used as comparative indicators under the stated operating point, rather than as unbiased absolute predictions.

The dataset and workflow support early-stage selection of binary (and potentially more complex) dielectric working fluids for compact heat exchangers and mini-/microchannel thermal management, where limited space, low fluid charge, and electrical safety are key constraints. Application areas include electronics and power-electronics cooling, HVAC&R components with confined internal passages, and compact laboratory- or process-scale heat-exchanger modules requiring a balance between heat-transfer performance, pressure-drop (pumping-power) penalties, and the target operating temperature range.

Limitations include the restriction to single-phase forced convection, use of a tube-derived correlation applied via the hydraulic diameter, and the simplified treatment of thermophysical properties at each temperature level. Further work should extend validation to additional operating points and consider rectangular-duct-specific laminar formulations, temperature-dependent properties, and joint heat-transfer/pressure-drop criteria for mixture down-selection.

Author Contributions: As shown directly in the system. All authors have read and agreed to the published version of the manuscript.

Funding: This research was funded by the National Science Centre, Poland, grant no. UMO-2025/57/B/ST8/00907. For the purpose of Open Access, the authors have applied a CC BY public copyright licence to the Author Accepted Manuscript (AAM) version arising from this submission.

Data Availability Statement: The original contributions presented in this study are included in the article. Further inquiries can be directed to the corresponding author.

Conflicts of Interest: The authors declare no conflicts of interest.

Nomenclature

Symbols

c_p	isobaric specific heat capacity (J·kg^{-1}·K^{-1})
D_h	hydraulic diameter, $D_h = 2w \cdot s/(w+s)$ (m)
G	mass flux, (kg·m^{-2}·s^{-1})
h	heat transfer coefficient (W·m^{-2}·K^{-1})
h_{corr}	correlation-based heat transfer coefficient (W·m^{-2}·K^{-1})
$h_{exp,mean}$	experimentally obtained mean heat transfer coefficient (W·m^{-2}·K^{-1})
I	electric current supplied to the heater (A)
k	thermal conductivity (W·m^{-1}·K^{-1})
L	minichannel length (m)

Nu	Nusselt number, $Nu = h \cdot D_h/k$
Nu_{corr}	correlation-based Nusselt number (–)
p	pressure (Pa)
Pr	Prandtl number, $Pr = \mu \cdot c_p/k$ (–)
q''	heat flux at the heated wall ($W \cdot m^{-2}$)
Re	Reynolds number, $Re = G \cdot D_h/\mu$ (–)
s	minichannel depth (m)
T	temperature (K)
w	minichannel width (m)
x	axial coordinate along the minichannel (m)
Greek letters	
ΔT_{cond}	temperature drop across the heater foil due to one-dimensional conduction $\Delta T_{cond} = q'' \cdot \delta/k_F$ (K)
Δh_{rel}	relative difference between $h_{exp,mean}$ and h_{corr} (%)
μ	dynamic viscosity (Pa·s)
μ_w	dynamic viscosity evaluated at the wall temperature (Pa·s)
ν	kinematic viscosity ($m^2 \cdot s^{-1}$)
ρ	density ($kg \cdot m^{-3}$)
δ	heater foil thickness (m)
Subscripts	
corr	value calculated from a correlation
exp	value obtained from experiment
F	foil (heater wall)
f	fluid (bulk)
in / out	inlet / outlet
max	maximum value
mean	mean (averaged) value
min	minimum value
Abbreviations	
EA	ethyl acetate
HFE	hydrofluoroether
IR	infrared thermography
LCT	liquid crystal thermography

References

1. von Westarp, W.G.; Jupke, A. Improved methodology for the measurement of vapor–liquid equilibria of binary mixtures with large boiling point differences via differential scanning calorimetry. *Thermochimica Acta* **2026**, 757, 180222. https://doi.org/10.1016/j.tca.2026.180222.
2. Aminian, A.; Celný, D.; Mickoleit, E.; Jäger, A.; Vinš, V. Ideal Gas Heat Capacity and Critical Properties of HFE-Type Engineering Fluids: Ab Initio Predictions of Cp,ig, Modelling of Phase Behaviour and Thermodynamic Properties Using Peng–Robinson and Volume-Translated Peng–Robinson Equations of State. *International Journal of Thermophysics* **2022**, 43, 87.
3. Urata, S.; Takada, A.; Murata, J.; Hiaki, T.; Sekiya, A. Prediction of vapour–liquid equilibrium for binary systems containing HFEs by using artificial neural network. *Fluid Phase Equilibria* **2002**, *199*, 63–78.
4. Wu, J.; Pan, Y.; Ren, J.; Li, Q. Exploring structure–property relationships of critical temperatures for binary refrigerant mixtures via group contribution and machine learning. *DeCarbon* **2025**, *9*, 100123. https://doi.org/10.1016/j.decarb.2025.100123.
5. Soria-Lopez, A.; Simal-Gandara, J.; Mejuto, J.C. Viscosity mixing rules and machine learning-based models for predicting the viscosity of liquid binary mixtures of aliphatic alkanes. *Journal of Molecular Liquids* **2025**, *437*, 1–11.
6. Muñoz-Rujas, N.; Aguilar, F.; Garcia-Alonso, J.M.; Montero, E.A. Thermodynamics of binary mixtures 1-ethoxy-1,1,2,2,3,3,4,4,4-nonafluorobutane (HFE-7200) + 2-propanol: High-pressure density, speed of sound and derivative properties. *Journal of Chemical Thermodynamics* **2019**, *131*, 630–647.
7. Muñoz-Rujas, M.; Bazile, J.P.; Aguilar, F.; Galliero, G.; Montero, E.; Daridon, J.-L. Speed of sound, density and derivative properties of binary mixtures HFE-7500 + diisopropyl ether under high pressure. *Journal of Chemical Thermodynamics* **2019**, *128*, 19–33.

8. Ogawa, H.; Karashima, S.; Takigawa, T.; Murakami, S. Excess molar enthalpies and volumes of binary mixtures of two hydrofluoroethers with hexane, benzene, ethanol, 1-propanol, or 2-butanone at T=298.15 K. *Journal of Chemical Thermodynamics* **2003**, *35*, 763–774.
9. Xu, R.; Zhang, C.; Chen, H.; Wu, Q.; Wang, R. Heat transfer performance of pulsating heat pipe with zeotropic immiscible binary mixtures. *International Journal of Heat and Mass Transfer* **2019**, *137*, 31–41.
10. Eissa, M.S.; Kotb, A.; Liu, L.; Wang, S. The prediction of binary zeotropic mixtures in-tube flow condensation—A generalized non-equilibrium heat transfer model. *Energy Conversion and Management* **2026**, *347*, 120562. https://doi.org/10.1016/j.enconman.2025.120562.
11. Tagliaferri, C.; Mazzei, L.; Lettieri, P.; Marzocchella, A.; Olivieri, G.; Salatino, P. CFD simulation of bubbling fluidized bidisperse mixtures: Effect of integration methods and restitution coefficient. *Chemical Engineering Science* **2013**, *102*, 324–334.
12. Verma, S.; Rani, M.; Lee, Y.; Maken, S. Thermophysical properties of binary mixtures of diethyl ether as oxygenate with cyclohexane and aromatic hydrocarbons. *Journal of Molecular Liquids* **2023**, *387*, 1–12.
13. Tsai, M.-Y.; Wu, Y.-Y.; Lin, L.-C. Transport properties of alcohol/water mixtures: Evaluation of molecular potentials. *Journal of Molecular Liquids* **2025**, *433*, 1–10.
14. Piasecki, A.; Maciejewska, B.; Piasecka, M.; Grabowski, M.; Grabowski, P. Evaluation of HFE-73DE/ethyl acetate mixtures for use in minichannel heat exchangers. *Energies* **2026**, *19*, 110. https://doi.org/10.3390/en19010110.
15. 3M™ Novec™ 7100 Engineered Fluid, Product Information. Available online: https://multimedia.3m.com/mws/media/199818O/3m-novec-7100-engineered-fluid.pdf (accessed 01.10.2025).
16. 3M™ Novec™ 7300 Engineered Fluid, Product Information. Available online: https://multimedia.3m.com/mws/media/338713O/3m-novec-7300-engineered-fluid.pdf (accessed 01.10.2025).
17. 3M™ Novec™ 73DE Engineered Fluid, Technical Data Sheet. Available online: https://multimedia.3m.com/mws/media/1479639O/3mtm-novectm-engineered-fluid-73de-tech-data-sheet.pdf (accessed 01.10.2025).
18. NIST Chemistry WebBook. Ethyl Acetate (CAS 141-78-6). Available online: https://webbook.nist.gov/cgi/cbook.cgi?ID=C141786 (accessed 01.10.2025).
19. Piasecka, M.; Piasecki, A.; Maciejewska, B. Liquid Crystal Thermography and Infrared Thermography Application in Heat Transfer Research on Flow Boiling in Minichannels. *Energies* **2025**, *18*, 940. https://doi.org/10.3390/en18040940
20. Piasecka, M.; Maciejewska, B.; Michalski, D.; Dadas, N.; Piasecki, A. Investigations of Flow Boiling in Mini-Channels: Heat Transfer Calculations with Temperature Uncertainty Analyses. *Energies* **2024**, *17*, 791. https://doi.org/10.3390/en17040791.
21. Sieder, E.N.; Tate, G.E. Heat Transfer and Pressure Drop of Liquids in Tubes. *Ind. Eng. Chem.* **1936**, *28*, 1429–1435. https://doi.org/10.1021/ie50324a027.
22. Shah, R.K.; London, A.L. *Laminar Flow Forced Convection in Ducts: A Source Book for Compact Heat Exchanger Analytical Data*; Academic Press: New York, NY, USA, 1978.